Journal of Saudi Chemical Society (2015) **19**, 265–273

King Saud University

Journal of Saudi Chemical Society

www.ksu.edu.sa
www.sciencedirect.com

ORIGINAL ARTICLE

3D QSAR, pharmacophore indentification studies on series of 1-(2-ethoxyethyl)-1H-pyrazolo [4,3-d]pyrimidines as phosphodiesterase V inhibitors

Prafulla Choudhari *, **Manish Bhatia**

Department of Pharmaceutical Chemistry, Bharati Vidyapeeth College of Pharmacy, Kolhapur 416013, Maharashtra, India

Received 2 December 2011; accepted 29 February 2012
Available online 19 March 2012

KEYWORDS

Molecular modeling;
k-Nearest neighbor molecular field analysis (kNN-MFA;
Multiple linear regression analysis;
Vlife MDS 3.5;
Phosphodiesterase 5;
Vascular smooth muscle relaxant;
3D QSAR

Abstract *Context:* In recent years phosphodiesterase V acts as an attractive target for cardiovascular drug design and QSAR techniques are helpful for the optimization of structural requirements for designing novel compounds.

Objective: The present communication deals with 3D-QSAR analysis of 1-(2-ethoxyethyl)-1H-pyrazolo[4,3-d]pyrimidines as phosphodiesterase V inhibitors.

Materials and methods: The multiple linear regression analysis and kNN-MFA analysis were carried out on 33 reported 1-(2-ethoxyethyl)-1H-pyrazolo[4,3-d]pyrimidines in Vlife MDS 3.5.

Results: The substitution of electron withdrawing groups in pyrazole ring and sterically less bulkier groups is important for the phosphodiesterase V inhibition indicated by both QSAR analyses.

Conclusion: The two different QSAR models are generated by using two different principles, both the models are showing similar results which indicate that this kNN-MFA technique can be utilized for cross validation of the results of multiple linear regression studies.

1. Introduction

Phosphodiesterase enzymes catalyze the conversion of cyclic GMP and cyclic AMP into the corresponding nucleotide monophosphates with the emergence of molecules like sildenafil and tadalafil. The phosphodiesterase 5 (PDE5) inhibition is now emerged as the most favorite tool for the treatment of erectile dysfunction in men. Large amount of research is carried out for the identification of new, selective PDE5 inhibitors and to investigate their usefulness in cardiovascular disorders to act as vascular smooth muscle relaxants. In human PDE5 is frequently observed in lungs, platelets, and vascular smooth muscles. PDE5 is specific for the cGMP, in its both catalytic sites, and in the two cGMP-binding allosteric sites (Sausbier et al., 2000; McAllister-Lucas et al., 1993; Chang et al., 2010; Tollefson et al., 2010; Yang et al., 2006). In PDE5 there are

* Corresponding author.
E-mail address: prafulla.choudhari@bharatividyapeeth.edu (P. Choudhari).

Peer review under responsibility of King Saud University.

Production and hosting by Elsevier

http://dx.doi.org/10.1016/j.jscs.2012.02.008

two cGMP-binding domains: (i) an N-terminal domain harboring a site for phosphorylation and (ii) a C-terminal catalytic domain of the enzyme (Chen et al., 2009, 2008; Matsumoto et al., 2003; Reffelmann and Kloner, 2009; Guazzi, 2008; Palmer et al., 2007; Srivani et al., 2007; Rotella, 2002). The catalytic domain of PDE5 is constituted by four major parts which includes three helical subdomains, an N-terminal cyclin-fold region, a linker region and a C-terminal helical bundle. The present communication deals with 3D QSAR (Fegade et al., 2009; Jhaa et al., 2009; Sharma and Sharma, 2010) analysis of 1-(2-ethoxyethyl)-1H-pyrazolo[4,3-d]pyrimidines derivatives by multiple linear regression and k-nearest neighbor molecular field analysis (kNN-MFA) for the designing of new phosphodiesterase 5 inhibitors with vascular smooth muscle relaxant activity.

2. Computational details

2.1. Dataset

A dataset of 33 compounds was taken from the published phosphodiesterase V inhibitors by Tollefson et al. (2010). The structures and their inhibitory activities are listed in Table 1. The inhibitory activity IC50 values were converted into the corresponding pIC50 (log 1/IC50) and used as dependent variables in the 3D-QSAR analyses. The whole dataset was

Table 1 The molecules under study.

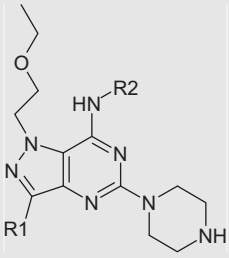

Sr. no.	R2	R1	3D QSAR by MLR			3D QSAR by kNN-MFA		
			Obs. Act	Pre. Act	Res	Obs. Act	Pre. Act	Res
1		Et	1.154902	0.976007	0.178895	1.154902	1.23208	−0.07718
2			0.39794	0.335082	0.062858	0.39794	0.463477	−0.06554
3		Et	1.154902	1.091625	0.063277	1.154902	1.22774	−0.07284
4	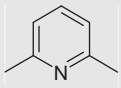	Me	0.187087	0.427347	−0.24026	0.187087	0.564074	−0.37699
5	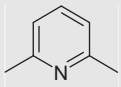	Et	0.180456	0.329883	−0.14943	0.180456	-0.63399	0.814449
6	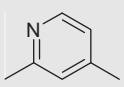	Me	−0.14613	−0.42503	0.278901	−0.14613	−0.35629	0.210165
7	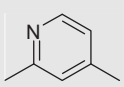	Et	0.420216	0.315386	0.10483	0.420216	0.102351	0.317865
8	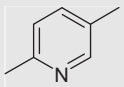	Et	−0.51851	0.630618	−1.14913	−0.51851	−0.27698	−0.24153
9		Et	−0.74036	0.204248	−0.94461	−0.74036	−0.15243	−0.58793

Table 1 (*continued*)

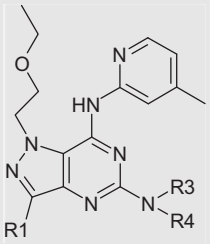

Sr. no.	NR3R4	R1	3D QSAR by MLR			3D QSAR by KNN-MFA		
			Obs. Act	Pre. Act	Res	Obs. Act	Pre. Act	Res
10	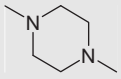	Me	−0.41497	−0.50069	0.085718	−0.41497	−0.34802	−0.06696
11	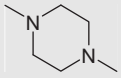	Et	0.05061	0.043787	0.006823	0.05061	−0.07732	0.127927
12	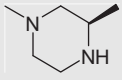	Et	−0.39794	−0.12422	−0.27373	−0.39794	−0.35668	−0.04126
13	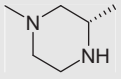	Et	−0.07918	−0.03801	−0.04117	−0.07918	−0.2384	0.159214
14	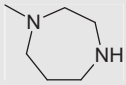	Et	0.119186	0.098904	0.020282	0.119186	−0.08439	0.203571
15	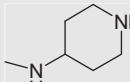	Me	−0.36173	−0.27329	−0.08844	−0.36173	0.039018	−0.40075
16	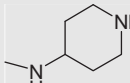	Et	0.69897	0.87657	−0.1776	0.69897	0.478146	0.220824
17	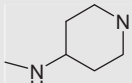	Et	0.142668	−0.04478	0.187449	0.142668	0.206722	−0.06405
18	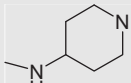	Et	−0.30103	−0.26987	−0.03116	−0.30103	−0.40652	0.105488
19	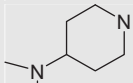	Et	1.060481	0.885741	0.17474	1.060481	0.1778	0.882681
20	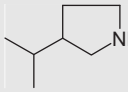	Et	0.376751	0.61674	-0.23999	0.376751	0.220577	0.156174
21	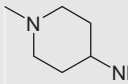	Me	−0.36173	−0.45437	0.09264	−0.36173	0.054078	−0.41581
22	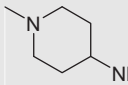	Et	0.107905	0.496674	−0.38877	0.107905	0.41973	−0.31183
23	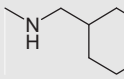	Me	0.455932	0.496674	−0.04074	0.455932	0.836395	−0.38046

(*continued on next page*)

Table 1 (*continued*)

Sr. no.	NR3R4	R1	3D QSAR by MLR			3D QSAR by KNN-MFA		
			Obs. Act	Pre. Act	Res	Obs. Act	Pre. Act	Res
24	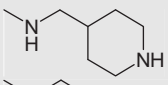	Et	1.958607	1.263955	0.694652	1.958607	1.65955	0.299057
25	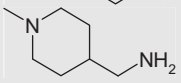	Me	1.154902	0.942938	0.211964	1.154902	1.27769	−0.12279
26	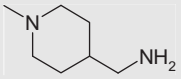	Et	2.154902	2.102652	0.05225	2.154902	1.55393	0.600972
27	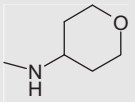	Me	−0.07918	0.011897	−0.09108	−0.07918	0.058994	−0.13818
28	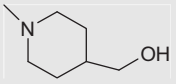	Et	1.154902	1.066985	0.087917	1.154902	0.74195	0.412952
29*	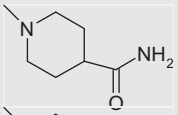	Me	0.721246	0.824059	−0.10281	0.721246	0.835285	−0.11404
30*	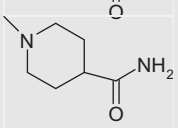	Et	1.09691	0.756023	0.340887	1.09691	1.18131	−0.0844
31*	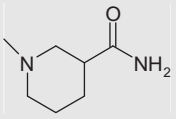	Et	1.09691	0.756023	0.340887	1.09691	1.18131	−0.0844
32*	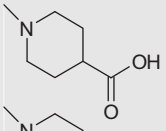	Me	1.30103	1.426039	−0.12501	1.30103	1.1549	0.14613
33*	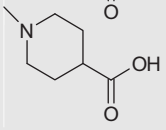	Et	1.39794	0.771842	0.626098	1.39794	−0.06902	1.466957

* Test set molecules.

randomly divided into a training set of 28 compounds and a test set of 5 compounds (asterisked molecules in Table 1). The training set was used to construct the 3D-QSAR models and the test set was used for the models validation.

2.2. Materials and methods

2.2.1. Ligand preparation

The structure of substituted derivatives was used as the template to 1-(2-ethoxyethyl)-1H-pyrazolo[4,3-d]pyrimidines built molecules in the dataset in Vlife MDS 3.5. All the structures were minimized using the standard Merck molecular force field (MMFF) with the distance dependant dielectric function and an energy gradient of 0.001 kcal/mol Å.

2.2.2. Molecular alignment

The molecules of the dataset were aligned by the template based technique, using the common structure of 1-(2-ethoxyethyl)-1H-pyrazolo [4,3-d]pyrimidines. The alignment of all the molecules on the template is shown in Fig. 1.

2.2.3. Descriptor calculation

Like many 3D-QSAR methods, a suitable alignment of given set of molecules was performed using the Vlife MDS 3.5 Engine. This was followed by the generation of a common rectangular grid around the molecules. The hydrophobic, steric and electrostatic interaction energies are computed at the lattice points of the grid using a methyl probe of charge +1. These interaction energy values are considered for relationship generation and utilized as descriptors to decide the nearness between

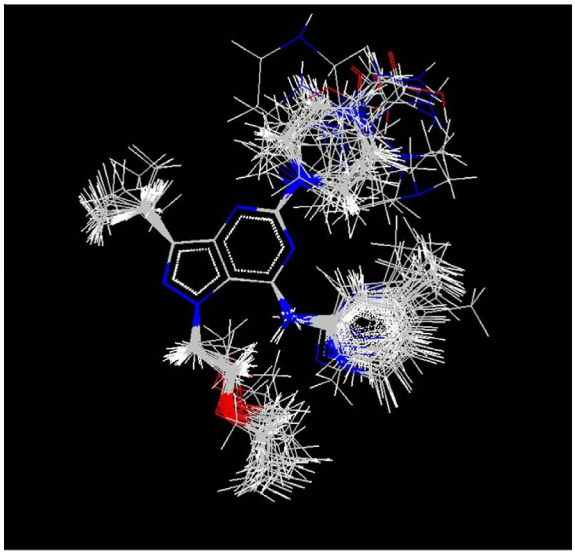

Figure 1 The alignment of molecules.

molecules. The term descriptor is utilized in the following discussion to indicate the field values at the lattice points.

2.3. 3D-QSAR studies using multiple linear regressions

Stepwise multiple regression (SMR) is a systematic approach for selecting useful variable and generating models. Stepwise forward–backward method from Vlife MDS was used as a variable selection method, with a cross correlation limit of 0.7 to eliminate highly inter-correlated variables and a variance cut-off of 0.5 to eliminate insignificant variables.

2.4. 3D-QSAR studies using kNN-MFA

The calculated fields of randomly selected 28 molecules used in the training set were considered as observations to generate the QSAR model using a stepwise variable selection (SW) kNN-MFA method. Plot of the kNN-MFA which shows the relative position and ranges of the corresponding important electrostatic/steric fields in the model provides the following guidelines for the design of new molecules.

2.4.1. kNN-MFA with stepwise variable selection method

This method employs the kNN classification principle combined with the stepwise variable selection procedure for the optimization of:

(i) The number of nearest neighbors (k) used to estimate the activity of each compound
(ii) Selection of variables from the original pool of all molecular descriptors (steric and electrostatic field at the lattice points) that are used to calculate the similarities between compounds (i.e., distances in near-dimensional descriptor space).

Further, a step-by-step search procedure that begins by developing a hypothetical pharmacophore (HP model) with a single independent variable and adds independent variables

Table 2 The selected MLR QSAR equations along with statistical parameters employed for model selection.

Model no.	QSAR model	*N*	r^2	q^2	*F* value	Pred r^2
A	pIC50 = 0.0051–0.1171(±0.0107)E_950 −7.8993 (±0.7621) S_304 −0.2045(±0.0325)E_1021 +0.0277 (±0.0081)E_941 +0.0876(±0.0290)S_1051	33	0.93	0.89	54.1315	0.8131

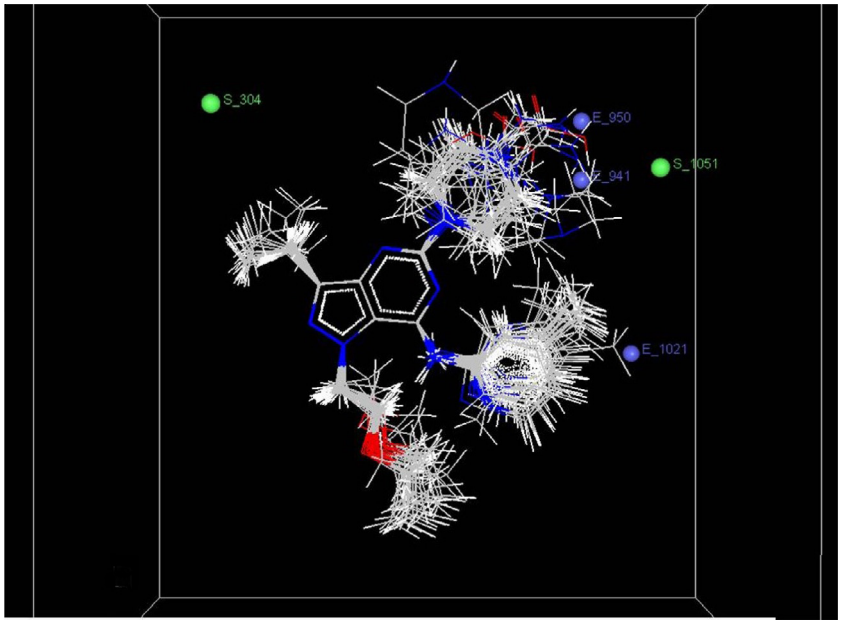

Figure 2 Field point for 3D-QSAR model A.

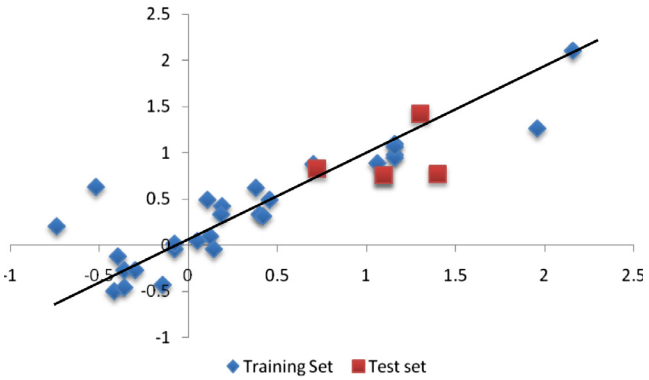

Figure 3 Correlation plot for 3D-QSAR model A.

one step at a time, examining the fit of the model at each step (using weighted k-nearest neighbor cross validation procedure) until there are no more significant variables remaining outside the model is included.

2.5. Pharmacophore modeling

Pharmacophore modeling was carried out using the MolSign module of Vlife MDS 3.5 software. Series of phosphodiesterase V inhibitors were first aligned on the active molecule. A pharmacophore model is a set of three-dimensional features that are necessary for bioactive ligands. Thus, it makes logical sense to align molecules based on the features that are responsible for bioactivity. The software was set to generate minimum four pharmacophoric features obtained keeping the tolerance limit at 10 Å. The maximum distance of 10 Å was kept between two features in pharmacophore identification studies. The average RMSD of the pharmacophore alignments of each two molecules is 0.055.

3. Results

In the present study, 28 molecules were used in the training set (Table 1) to derive kNN-MFA 3D-QSAR models with the

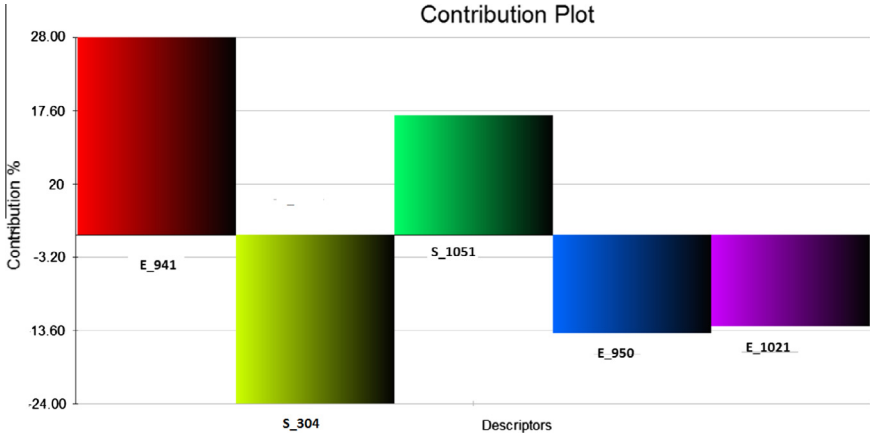

Figure 4 Contribution chart model A.

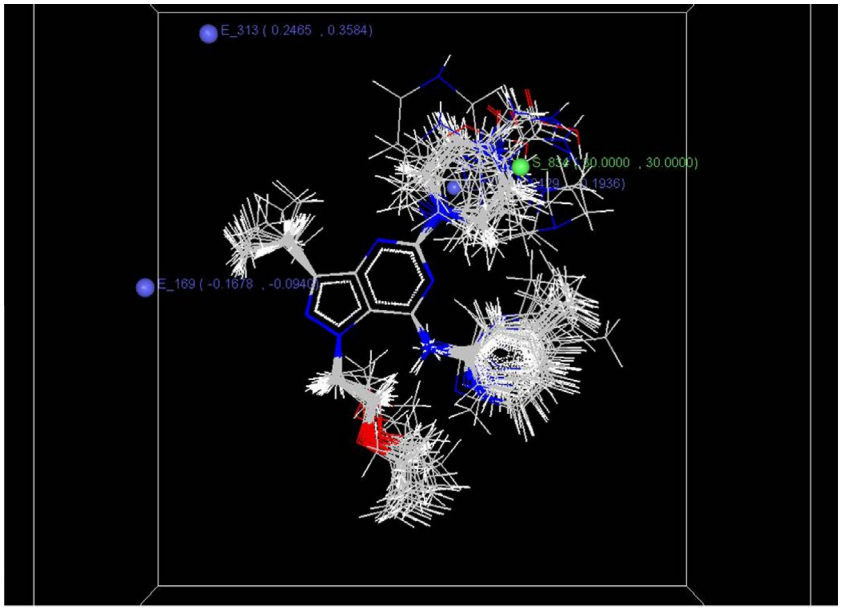

Figure 5 Field point for 3D-QSAR model C.

Table 3 The selected kNN-MFA QSAR equations along with statistical parameters employed for model selection.

Model no.	Selected descriptors	*N*	Descriptor range	q^2	Pred r^2	Degree of freedom
C	E_722 E_653 S_834 E_313 E_169	33	E_722 −0.2429 to −0.1936 S_834 30.0000–30.0000 E_313 0.2465–0.3584 E_169 −0.1678 to −0.0940	0.79	0.72	19

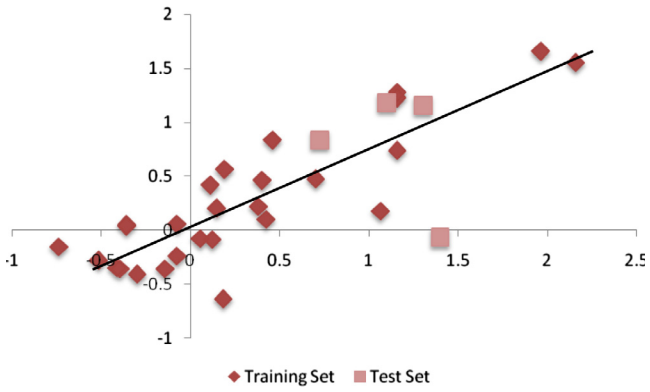

Figure 6 Correlation plot for 3D-QSAR model C.

number of field grid points being not more than seven per model. To evaluate the predictive ability of generated 3D-QSAR models, a test set of 5 molecules with regularly distributed biological activities was used (Table 1). On successful runs of MLR and kNN-MFA, different sets of equations were generated and these equations were further analyzed statistically to select the best model, as shown in Table 2, two models were selected after screening various combinations of different descriptors.

4. Discussion

4.1. Interpretation of 3QSAR model (MLR)

The optimum structural requirements of pyrazolo[4,3-d]pyrimidines analogs for phosphodiesterase V inhibitors were obtained in the form of the 3D descriptors of model A (Mbarki et al., 2011). The r^2 value for model A was 0.93 (Fig 2). Model A shows the first model which is selected on the basis of statistical coefficients like r^2 (0.93) and Pred r^2 (0.89). The contributing descriptors for model A are E_950, S_304, E_1021, E_941 and S_1051 which are nothing but the electrostatic and steric interactions at that lattice point. The electrostatic interaction at the lattice points E_950 and E_1021 is negatively contributing that means the substitution of electron withdrawing groups on the aromatic ring at r^2 can yield potent phosphodiesterase V inhibitors, also the steric interaction at the lattice point 304 is also negatively contributing that means the substitution at the R1 should be small, the increase in chain length could decrease the activity. The electrostatic interaction at the lattice point 941 and steric interaction at lattice point 1051 are positively contributing so the substitution favoring this interaction at that lattice point could yield an active molecule. The correlation plot and contribution plots for model A are given in Figs. 3 and 4, respectively.

4.2. Interpretation of 3QSAR model (kNN-MFA)

4.2.1. Electrostatic field

(a) Negative range indicates that negative electrostatic potential is favorable for increase in the activity and hence a relatively more electronegative substitution is preferred in that region.
(b) Positive range indicates that positive electrostatic potential is favorable for increase in the activity and hence a relatively less electronegative substitution is preferred in that region.

4.2.2. Steric field

(a) Negative range indicates that negative steric potential is favorable for increase in the activity and hence a relatively less bulky substituent group is preferred in that region.
(b) Positive range indicates that positive steric potential is favorable for increase in the activity and hence a relatively more bulky substituent group is preferred in that region.

Model C is the second model which is selected on the basis of statistical coefficients like q^2 (0.79) and Pred r^2 (0.72). The contributing descriptors for this model are E_722 (−0.2429 to −0.1936), S_834 (30.0000–30.0000), E_313 (0.2465–0.3584) and E_169 (−0.1678 to −0.0940). The negative range of the E_722 (−0.2429 to −0.1936) and E_169 (−0.1678 to −0.0940) (Fig 5) indicates that the substitution involving electron deficient group is preferred in that region that is on R2 and R1, also the positive contribution of S_834 (30.0000–30.0000) indicates the substitution of bulkier groups with less electron density that could yield more active molecules. The lattice point at E_313 (0.2465–0.3584) is positively contributing so the substitutions

Table 4 Results of pharmacophore identification studies.

Sr. no.	Pharmacophoric features	Distances (Å)
1	Positive ionizable–aromatic	7.806
2	Positive ionizable–hydrogen bond donor	7.094
3	Positive ionizable–hydrogen bond acceptor	5.142
4	Hydrogen bond acceptor–hydrogen bond acceptor	2.341
5	Hydrogen bond acceptor–hydrogen bond donor	2.731
6	Hydrogen bond donor–aromatic	5.091
7	Hydrogen bond acceptor–hydrogen bond donor	3.231
8	Hydrogen bond acceptor–aromatic	6.258
9	Hydrogen acceptor–positive ionisable	2.412
10	Hydrogen acceptor–aromatic	5.971

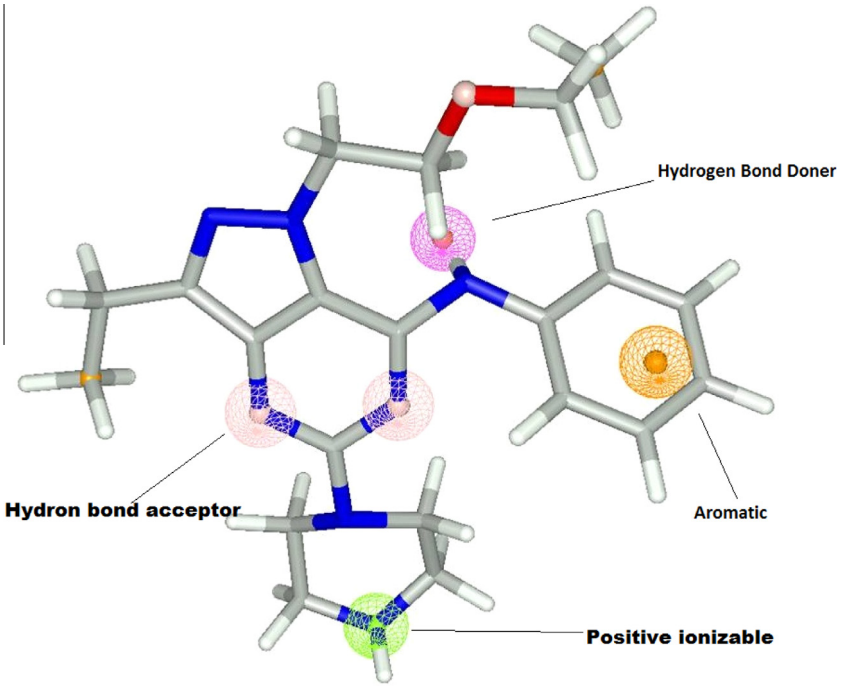

Figure 7 Pharmacophore features of molecules.

which are increasing the electron density around these lattice points could give more potential inhibition. The negative range at the lattice point E_169 (−0.1678 to −0.0940) indicates the importance of substitution of electron withdrawing groups in pyrazole ring which can stabilize the ring and also increase the activity of the molecules (Table 3). The correlation plot for model C is given in Fig. 6.

4.2.3. Pharmacophore identification studies using Vlife MDS 3.5
A set of pharmacophore hypothesis was generated using the mole sign module of Vlife MDS 3.5 on the reported inhibitors of phosphodiesterase V. Each hypothesis was found to contain common features like hydrogen bond donor, hydrogen bond acceptor, and positive ionizable, aromatic. Results of pharmacophore identification studies revealed that the hydrogen bond donor, hydrogen bond acceptor, positive ionizable, aromatic features are important for the activity. The results of pharmacophore identification studies are given in Table 4 and Fig. 7.

5. Conclusion

In this work we identified the structural requirement of 1-(2-ethoxyethyl)-1H-pyrazolo [4,3-d] pyrimidines for the inhibition of phosphodiesterase V. The two different QSAR models are generated by using two different principles, both the models are showing similar results which indicate that this kNN-MFA technique can be utilized for cross validation of the results of multiple linear regression studies.

Acknowledgment

The authors are thankful to Dr. H.N. More, Principal Bharati Vidyapeeth College of Pharmacy, Kolhapur, for providing facilities to carry out the research work.

References

Chang, T.T., Huang, H.J., Lee, K.J., Yu, H.W., Chen, H.Y., Tsai, F.U., Sun, Mao-Feng, Chen, Calvin Yu-Chian, 2010. Key features for designing phosphodiesterase-5 inhibitors. J. Biomol. Struct. Dyn. 28, 309–321.

Chen, G., Wang, H., Robinson, H., Cai, J., Wan, Y., Ke, H., 2008. An insight into the pharmacophores of phosphodiesterase-5 inhibitors from synthetic and crystal structural studies. Biochem. Pharm. 75, 1717–1728.

Chen, C., Chang, Y., Bau, D., Huang, H., Tsai, F., Tsai, C., Chen, C.Y., 2009. Discovery of potent inhibitors for phosphodiesterase 5 by virtual screening and pharmacophore analysis. Acta Pharmacol. Sin. 30, 1186–1194.

Fegade, J.D., Rane, S.S., Chaudhari, R.Y., Patil, V.R., 2009. 3D-QSAR study of benzylidene derivatives as selective cyclooxygenase-2-inhibitors. Digest J. Nanomater. Biostruct. 4, 145–154.

Guazzi, M., 2008. Clinical use of phosphodiesterase-5 inhibitors in chronic heart failure. Circ. Heart Fail. 1, 272–280.

Jhaa, K.K., Samadc, A., Kumar, Y., Shaharyar, M., Khosad, R., Jaina, J., Bansald, S., 2009. 3D QSAR studies of 1,3,4-oxadiazole derivatives as antimycobacterial agents. IJPR 8, 163–167.

Matsumoto, T., Kobayashi, T., Kamata, K., 2003. Phosphodiesterases in the vascular system. J. Smooth Muscle Res. 39, 67–86.

Mbarki, S., Dguigui, K., Hallaoui, M.E., 2011. Construction of 3D-QSAR models to predict antiamoebic activities of pyrazoline and dioxazoles derivatives. J. Mater. Environ. Sci. 2, 61–70.

McAllister-Lucas, L.M., Sonnenburg, W.K., Kadlecek, A., Seger, D., Trong, H.L., Colbran, J.L., Thomas, M.K., Walsh, K.A., Francis, S.H., Corbin, J.D., Beavo, J.A., 1993. The structure of a bovine lung cGMP-binding, cGMP-specific phosphodiesterase deduced from a cDNA clone. J. Biol. Chem. 268, 22863–22873.

Palmer, M.J., Bell, A.S., Fox, D.N.A., Brown, D.G., 2007. Design of second generation phosphodiesterase 5 inhibitors. Curr. Top. Med. Chem. 7, 405–419.

Reffelmann, T., Kloner, R.A., 2009. Phosphodiesterase 5 inhibitors: are they cardioprotective. Cardiovasc. Res. 83, 204–212.

Rotella, D.P., 2002. Phosphodiesterase 5 inhibitors: current status and potential applications. Drug Discov. 1 (2002), 674–682.

Sausbier, M., Schubert, R., Voigt, V., Hirneiss, C., Pfeifer, A., Korth, M., Kleppisch, T., Ruth, P., Hofmann, F., 2000. Mechanisms of NO/cGMP-dependent vasorelaxation. Circ. Res. 87, 825–830.

Sharma, M.C., Sharma, S., 2010. 3D-quantitative structure–activity relationship analysis of some 2-substituted halogenbenzimidazoles analogues with antimycobacterial activity. Int. J. ChemTech. Res. 2, 606–614.

Srivani, P., Srinivas, E., Raghu, R., Narahari Sastry, G., 2007. Molecular modeling studies of pyridopurinone derivatives potential phosphodiesterase 5 inhibitors. J. Mol. Graph. Model. 26, 378–390.

Tollefson, M.B., Acker, B.A., Jacobsen, E.J., Hughes, R.O., Walker, J.K., Fox, D.N.A., Palmer, M.J., Freeman, S.K., Yu, Y., Bond, B.R., 2010. 1-(2-Ethoxyethyl)-1H-pyrazolo[4,3-d]pyrimidines as potent phosphodiesterase 5 (PDE5) inhibitors. Bioorg. Med. Chem. Lett. 20, 3120–3124.

Yang, G.F., Lu, H.T., Xiong, Y., Zhan, C.G., 2006. Understanding the structure–activity and structure–selectivity correlation of cyclic guanine derivatives as phosphodiesterase-5 inhibitors by molecular docking, CoMFA and CoMSIA analyses. Bioorg. Med. Chem. 14, 1462–1473.